PCCP

Improvement of thermoelectric efficiency of polyaniline molecular junction by doping process

Journal:	*Physical Chemistry Chemical Physics*
Manuscript ID:	CP-ART-03-2015-001263.R1
Article Type:	Paper
Date Submitted by the Author:	08-Apr-2015

Complete List of Authors:	Golsanamlou, Zahra; University of Guilan, Bagheri Tagani, Meysam; University of Guilan, Rahimpour Soleimani, Hamid; University of Guilan,

ARTICLE TYPE www. rsc.org/xxxxxx | XXXXXXXX

Improvement of thermoelectric efficiency of polyaniline molecular junction by doping process†

Zahra Golsanamlou,[a] Meysam Bagheri Tagani,*[a] and Hamid Rahimpour Soleimani[a]

Received Xth XXXXXXXXXX 20XX, Accepted Xth XXXXXXXXX 20XX
First published on the web Xth XXXXXXXXXX 200X
DOI: 10.1039/b000000x

Thermoelectric properties of polyaniline molecular junction with face center cubic electrodes are investigated using Green function formalism in linear response regime in the presence of doping process. Doping gives rise to the increase of thermopower and figure of merit (ZT) and the decrease of electrical conductance as found experimentally in the work of Li et al. (Synthetic Metals 160 (2010) 1153-1158). We also find that the ZT increases by molecular length in short polyanilines. [Golsanamlou *et al.,Physical Chemistry Chemical Physics* , 2000, **35**, 3523].

1 Introduction

1.0.0.1 Conducting polymers and their derivatives, have been vastly investigated theoretically and experimentally in the last decades, because of the striking features like easy synthesis, good conductance, price and stability [1–5]. Also, the different properties of polymers can be modified by doping process. Among these polymers polyaniline (PANI) is a good choice for doping with protonic acids such as HCl, HF, H_2SO_4, $HClO_4$,... due to low cost, notable conductivity, new optical properties [6–9] and stability in the air and humidity [10]. During the reaction of PANI with acids, different numbers of positive charges are induced in the lattice but the number of π-electrons is constant.

1.0.0.2 The transport properties of PANI samples in low temperature were investigated by M. Ghosh et al. They obtained that the resistivity of the protonated PANI with HCl has weaker dependence to temperature [11]. J. H. Jung et al. studied the electrical, magnetic and structural properties of different Littium-salt-doped PANI samples. They found that the samples with higher dc conductivity have higher density of sates and are independent of temperature [12].

1.0.0.3 In the recent years, the using of molecular devices has been widely spread and the waste of electrical energy has became one of the major challenges about the devices. Therefore, scientists have studied the possibility of the conversion of generated thermal energy to electrical energy via thermoelectric properties of the devices. So the investigation of thermoelectric properties of the molecular junction has been interested lately from two points of view: power generation and saving energy [13–15]. The thermal efficiency of the system is defined by a dimensionless quantity that named figure of merit: $ZT = \frac{S^2 G_e T}{\kappa}$, where, S, G_e , κ and T are thermopower, electrical conductance, thermal conductance and applied temperature, respectively. $\kappa = \kappa_{el} + \kappa_{ph}$ that κ_{el} is electron thermal conductance and κ_{ph} denotes the phonon thermal conductance that is ignorable for organic molecular junctions due to existence of considerable mismatch between density of states of the phonons in metallic electrodes and the phonon modes of the molecule [16]. PANI compounds have thermal properties like specific heat capacities and thermal conductivities that cause them as a good candidate for thermoelectric investigations [17,18]. High electrical conductivity and acceptable ZT of protonic acid-doped PANI films that were comparable with inorganic thermoelectric materials were obtained in the work of Hu Yan et al [19]. In another work, thermoelectric power and electrical conductance of the PANI prepared in ionic liquid have been studied experimentally. Results show that PANI is a p-type semiconductor polymer [20].

1.0.0.4 In this work, we study the thermoelectric properties of PANI molecular junction in presence and absence of dopants using non-equilibrium Green function formalism (NEGF) in linear response regime. Polyaniline in presence of acids like CH_3SO_3H, HCl, H_2SO_4,... and ionic liquid can be completely protonated and converted to emeraldine salt form, highly stable form of PANI in experimental works like [10,21]. Therefore, we consider the emeraldine salt form in present work as acid doped PANI (See Figs. 1a and b). The PANI is located between two semi-infinite three dimensional face center cubic (FCC) electrodes and a tight-binding (TB) model is used for describing of the Hamiltonian of the molecule. Conditions leading to improvement of figure of merit are also investigated. To the best of our knowledge few theoretical works about transport features of doped PANI junction were per-

[a] *Department of physics, University of Guilan, P.O.Box 41335-1914, Rasht, Iran E-mail: m_bagheri@guilan.ac.ir*

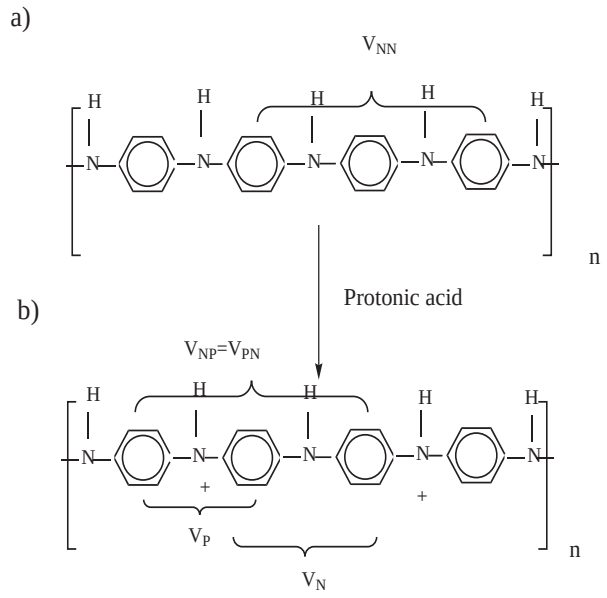

Fig. 1 a) Undoped polyaniline, b) Doped polyaniline.

formed until now and the investigation on thermoelectric efficiency of the prtonated PANI junctions using NEGF has not been reported. Our results are comparable with the experimental works. The paper is organized as follows: the theoretical method is expressed in Sec.2 and the numerical results are presented in Sec.3. At the end of the paper, we give some sentences as a conclusion.

2 Model and Formalism

2.0.0.5 We explain our formalism by writing the total Hamiltonian of the system as follows:

$$H = H_C + H_{mol} + H_T \tag{1}$$

where, H_c and H_T are the Hamiltonian of the electrodes and coupling of the molecule to the electrodes, respectively. H_{mol} describes the Hamiltonian of the PANI:

$$H_{mol} = \sum_i \{\varepsilon_i d_i^\dagger d_i + V_{2L} d_i^\dagger d_{i-2} + V_L d_i^\dagger d_{i-1} + V_R d_i^\dagger d_{i+1} + V_{2R} d_i^\dagger d_{i+2}. \tag{2}$$

In the above Hamiltonian ε_i is the on-site energy of a benzenoid ring and is set to -7.5 eV that is equal in two considered states (undoped and doped states). V_{2L} and V_{2R} are the hopping integral for the next neighbor rings. We assume V_{2L}=V_{2R}=V_{PN}=-0.07 eV for doped PaNI and V_{2L}=V_{2R}=V_{NN}=-0.075 eV for undoped PANI. The hopping integrals between two adjacent rings are V_L and V_R. If the benzenoid rings are connected by protonated nitrogen, that is alternately appeared in PANI by doping process, V_L or V_R is equal to $V_P = 0.7$ eV, otherwise V_L or V_R is considered as $V_N = 0.73$ eV [22,23]. Figs. 1a and b show these parameters for undoped and doped PANI, respectively. The Hamiltonian of the electrodes can be expressed as:

$$H_C = \sum_k \varepsilon_0 c_k^\dagger c_k - t(c_k^\dagger c_{k+1} + h.c), \tag{3}$$

where, the ε_0 is the on-site energy in the electrode and t is the hopping parameter between nearest neighbor atoms in the electrodes. The electron tunneling from the FCC electrodes to the molecule is as follows:

$$H_T = \sum_i t_{c(k,i)} (c_k^\dagger d_i + h.c). \tag{4}$$

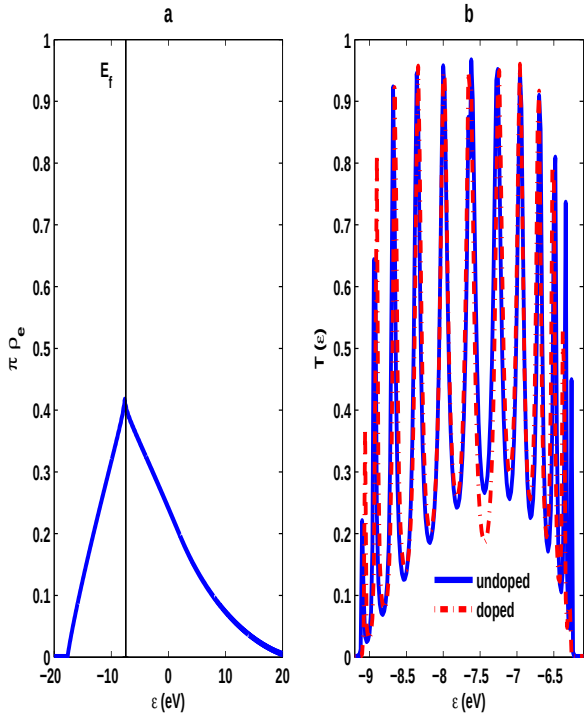

Fig. 2 a) The local density of states of the electrode at the top site on the surface versus energy, $\rho_e(E) = -1/\pi \int_{-\pi}^{\pi} (g_{s(\alpha)}) dk_x dk_y$ where, k_x and k_y are the wave vector in x and y directions, respectively. b)Energy dependent Transmission coefficient in doped and undoped polyaniline molecular junctions, n=3.

Here, $t_{c(k,i)} = t_c$ denotes coupling strength between the molecule and metallic electrodes. We assume only one point of the electrodes is connected to the ending points of the molecule in both sides which means the molecule is coupled to on top site of the electrode and $t_c = -1$ eV. The retarded

Green function of the system can be expressed as [24]:

$$G^r(\varepsilon) = [(\varepsilon + i0^+)I - H_{mol} - \Sigma_L(\varepsilon) - \Sigma_R(\varepsilon)]^{-1}, \quad (5)$$

where, 0^+ is an infinitesimal value. $\Sigma_{\alpha(=LorR)}(\varepsilon)$ expresses the self-energy function that describes the effect of semi-infinite metallic electrodes on the molecule and is defined as: $\Sigma_L = \tau^{\dagger}_{c,L} g_L \tau_{c,L}$ and $\Sigma_R = \tau_{R,c} g_R \tau^{\dagger}_{R,c}$ where, g_L and g_R are surface Green functions for the left and right FCC electrodes, respectively, which are calculated by procedure introduced in [25]. Fig. 2a shows the local density of states of the electrode at the top site on the surface which is comparable with the Fig.1 in [25]. According to the energy levels of the molecule after coupling, we choose the $E_f = -7.47$ as a Fermi energy of the electrodes located between the HOMO-LUMO gap. Also, the $\varepsilon_0 = -7.6$ eV and $t = -2.5$ eV are considered as on-site energy and hopping parameter of the electrodes, respectively. The interaction of PANI with FCC electrodes is studied in experimental works like [26,27]. The transmission coefficient of the electron transport from the left electrode to the right one is given by:

$$T(\varepsilon) = Tr[\Gamma_L(\varepsilon) G^r(\varepsilon) \Gamma_R(\varepsilon) G^a(\varepsilon)] \quad (6)$$

where, the broadening matrix ($\Gamma_\alpha(\varepsilon)$) is the imaginary part of the self-energy:

$$\Gamma_\alpha = -2Im(\Sigma_\alpha). \quad (7)$$

Fig. 2b indicates the transmission coefficient of the junction for undoped and doped PANI junctions. A renormalization in energy levels of the system is observed in presence of doping process.

To obtain thermoelectric coefficients, we need to consider the charge and heat currents using the Keldysh nonequilibrium Green function formalism as follows, respectively [24,28]:

$$I = \frac{2e}{h} \int d\varepsilon [f_L(\varepsilon) - f_R(\varepsilon)] T(\varepsilon), \quad (8a)$$

$$Q = \frac{2}{h} \int d\varepsilon (\varepsilon - \mu_L) [f_L(\varepsilon) - f_R(\varepsilon)] T(\varepsilon), \quad (8b)$$

where, $f_\alpha(\varepsilon) = [1 + exp((\varepsilon - \mu_\alpha)/kT_\alpha)]^{-1}$ is the Fermi-Dirac distribution function of electrode α, T_α and μ_α denote the temperature and chemical potential of electrode α, respectively. In this work the thermoelectric properties of the system are studied in linear response regime in which the charge and heat currents are expanded by induced voltage drop, ΔV, and temperature gradient, ΔT, to the first order as bellow:

$$I = e^2 L_0 \Delta V + \frac{e}{T} L_1 \Delta T, \quad (9a)$$

$$Q = e L_1 \Delta V + \frac{1}{T} L_2 \Delta T, \quad (9b)$$

where

$$L_n = -\frac{1}{h} \int d\varepsilon (\varepsilon - \mu)^n \frac{\partial f}{\partial \varepsilon} T(\varepsilon). \quad (10)$$

Thermopower is calculated in absence of current ($I = 0$) and defined as the ratio of induced voltage drop to the applied temperature gradient. Therefore, $S = -\frac{1}{eT}\frac{L_1}{L_0}$. The electrical conductance, G_e, thermal conductance, κ, and figure of merit are given by:

$$G_e = e^2 L_0, \quad (11a)$$

$$\kappa_{el} = \frac{1}{T}[L_2 - \frac{L_1^2}{L_0}], \quad (11b)$$

$$ZT = \frac{S^2 G_e T}{\kappa_{el} + \kappa_{ph}} \quad (11c)$$

The electron-phonon coupling is weak in organic molecules, so we can write ZT as follows [16]:

$$ZT = ZT_{el} \frac{1}{1 + \kappa_{ph}/\kappa_{el}}, \quad (12)$$

where,

$$ZT_{el} = (\frac{L_0 L_2}{L_1^2} - 1)^2. \quad (13)$$

Here, $\kappa_{ph} = \kappa_0 T_{ph}$ that $\kappa_0 = (\pi^2/3)(k_B T/h)$ denotes the thermal conductance quantum [29] and T_{ph} is the phonon transmission probability. The Debye frequency in the metal electrode is typically smaller than the lowest vibrational mode of an organic molecule that causes a big mismatch in vibrational spectra suppressing the phonon transmission in the junction [30]. In other words, this spectral overlap of phonon modes between the two parts of the junction is small, that results $T_{ph} \ll 1$ and we can consider $ZT \approx ZT_{el}$ [16]. We focus on the electron transport, so the thermal energy carried by electrons is just regarded. In our work we consider the temperatures above 60k that in these temperatures the phonon thermal conductance is approximately constant [31]. Therefore with considering phonon thermal conductance, a small constant term is added to κ_{el} as κ_{ph} and the real value of ZT has a bit reduction. Furthermore, the linear dependence of thermopower of molecular junctions on the length, observed in the experiments [32,33], shows that the phonons have no important role and transport is ballistic. So in this work, we obtain the maximum value of ZT for the molecular junction and ignor the phonon thermal conductance.

3 Results and Discussion

In the first part of this section, we consider temperature and doping dependence of thermoelectric coefficients of PANI junction. Figs. 3a and c shows the electrical and electron thermal conductances in presence and absence of doping process versus temperature, respectively. It is obvious that the conductances are reduced by dopants. In the case of G_e the peak-dip distance increases in presence of dopants due to renormalization in energy levels of the molecule, See the Fig. 3b and

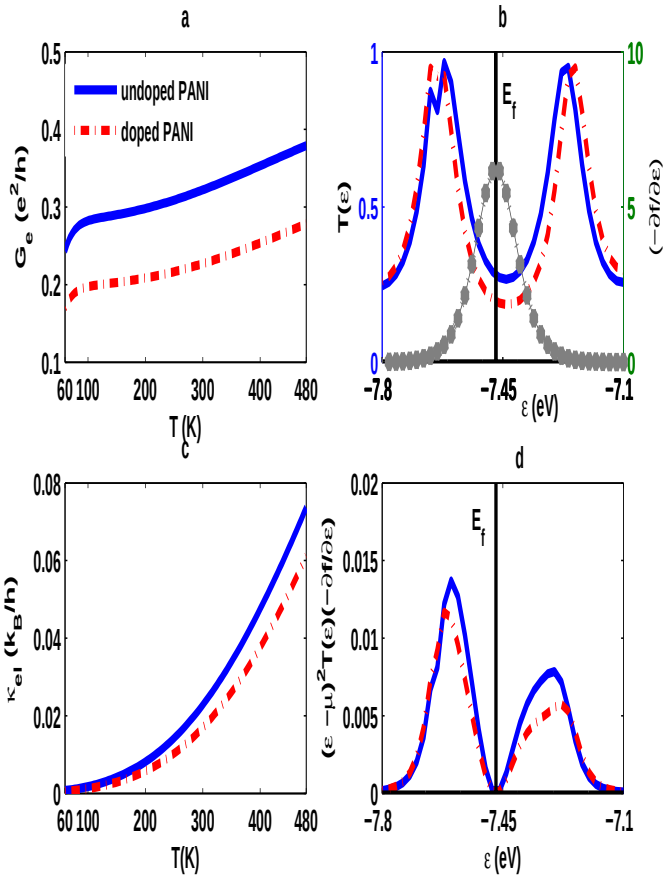

Fig. 3 a) Electrical conductance versus temperature, b) transmission coefficient peaks in vicinity of HOMO-LUMO gap, Fermi derivative is in gray, c) electron thermal conductance as a function of temperature and d) $(\varepsilon-\mu)^2(-\frac{\partial f}{\partial \varepsilon})T(\varepsilon)$ in vicinity of the gap for T=480k. All figures are drawn for undoped and doped PANI junctions, $E_f=-7.47$ eV, n=3.

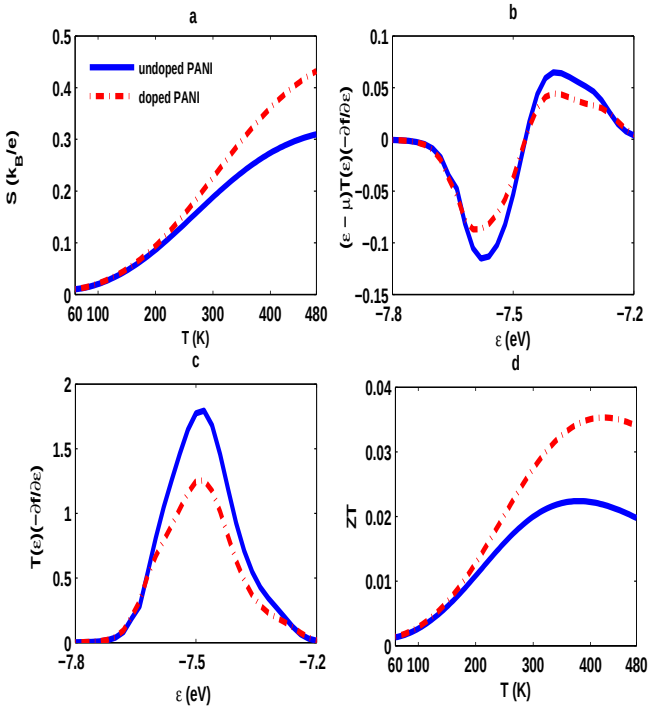

Fig. 4 a) Temperature dependance thermopower, b) $(\varepsilon-\mu)(-\frac{\partial f}{\partial \varepsilon})T(\varepsilon)$, c) $(-\frac{\partial f}{\partial \varepsilon})T(\varepsilon)$ and d) figure of merit versus temperature in both doped and undoped PANI, $E_f=-7.47$ eV, n=3. b) and c) are plotted for T=480k.

Fig. 2b. Threfore, it can be inferred that the protonate atoms (or ions) act as a potential barrier for the transport. The electron thermal conductance has two significant terms: L_2 and L_1/L_0. Our investigations reveal that the importance of L_1/L_0 is very less than L_2, so we focus on behavior of L_2. As it is observed from Fig. 3d, $(\varepsilon-\mu)^2(-\frac{\partial f}{\partial \varepsilon})T(\varepsilon)$ is more for undoped PANI junction. In this Fig. the height of peak located near the HOMO level is more than LUMO one, because the Fermi level is near to the HOMO level and transmission coefficient is asymmetric with respect to E_f.

3.0.0.6 Our results show that the thermopower increases in doped PANI, see Fig. 4a. The thermopower is the ratio of L_1/L_0, so it is necessary to study the manner of the $(\varepsilon-\mu)(-\frac{\partial f}{\partial \varepsilon})T(\varepsilon)$ and $(-\frac{\partial f}{\partial \varepsilon})T(\varepsilon)$ to clarify the changes of thermopawer, see the Figs. 4b and c, respectively. Figs show that although the magnitude of L_1 and L_0 is more in undoped case, their ratio is bigger in doped one. Fig. 4d represents the figure of merit of the molecular junction in the presence and absence of dopants as a function of temperature. The thermopower has the most effect on ZT (order 2), therefore, ZT in doped case is bigger than the other. It is obvious from the Fig. 4d, the presence of dopants has improved the thermoelectric efficiency of the junction. Our results, the decrease of the G_e, increase of S and ZT in acid-doped PANI versus temperature, are confirmed by the experimental work of Li et al. [34]. If we consider the phonon thermal conductance in our work, ZT has the reduction almost one order of magnitude [31]. The electrical and electron thermal conductances increase by temperature enhancement because the Fermi derivative is broadened with temperature and the more part of transmission coefficient peaks can be covered by $(-\frac{\partial f}{\partial \varepsilon})$. The increase of thermopower with temperature is resulted from the enhancement of asymmetry in L_1 with temperature increase.

3.0.0.7 The effect of increasing of the molecular length on thermoelectric coefficients of the doped PANI junction versus

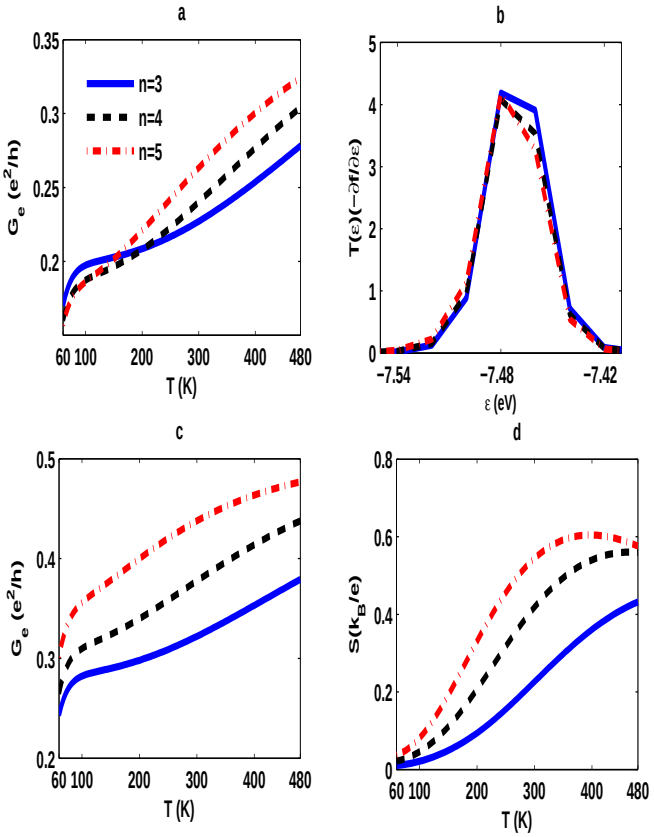

Fig. 5 a) Temperature dependance electrical conductance for different lengths of doped PANI, b) $(-\frac{\partial f}{\partial \varepsilon})T(\varepsilon)$ in T=110k, c) Electrical conductance versus temperature for different lengths of undoped PANI, and d) thermopower as a function of temperature for different lengths of doped PANI.

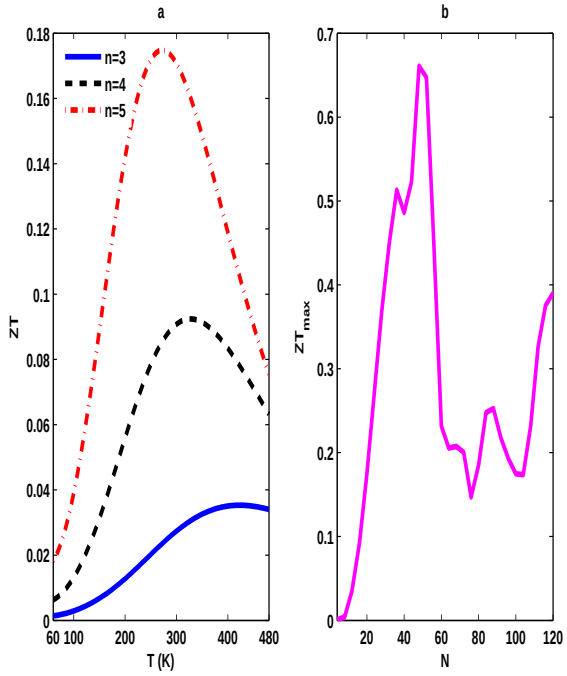

Fig. 6 a) Temperature dependence figure of merit for different lengths of doped PANI junction, b) The maximum of figure of merit of the junction as a function of molecular rings. $E_f = -7.47$ eV and $N/4 = n$

temperature is observed in Figs. 5 and 6 except Fig. 5c which belongs to undoped state. With increasing of the molecular length, the number of π-electrons in the molecule increases giving rise to a renormalization of molecular levels, and as a consequence the distance between the energy levels of the molecule decreases [35,36]. Hence, more molecular energy levels can be covered by temperature window $(-\frac{\partial f}{\partial \varepsilon})$, and as a result, the thermoelectric coefficients increase. On the other hand, with enhancement of temperature the thermoelectric coefficients increase in each PANI length. The increase of thermopower with length was reported in the work of Malen et al. [37]. It is interesting to note that the dependence of electrical conductance on the length is strongly related to the temperature. In low temperatures (less than 150k) the G_e is reduced by increase of length, but its magnitude becomes directly dependent on the length in higher temperatures. It results from the shape of the transmission and broadening of the Fermi derivative, see the Figs. 5a and b. In the case of undoped PANI, as it is observed from Fig. 5c, the electrical conductance has uniform increase with length. The sign of thermopower determines the kind of carrier dominant in transport mechanism and location of the Fermi level. It can be found from positive value for the thermopower in all considered lengths in Fig. 5d that the main carriers in transport mechanism are holes and the Fermi level of the electrode is near to the HOMO. As it is observed from Fig. 6a, ZT increases in considered length. In some experimental works like [30] the thermal conductance does not increase with length even it has a reduction with molecular length for alkanedithiol self-assembled monolayers. On the other hand, if thermal conductance has the increase by molecular length, we expect that the increase of numerator in ZT is much greater than increase of denominator and finally the ZT increases by length enhancement. The Fig. 6b represents that maximum of ZT versus temperature in each considered length is linearly dependent on the length until n=9, and then, it oscillates with length enhancement.

3.0.0.8 *I*n last part of the work, we examine the effect of displacement of chemical potential of the electrodes on thermoelectric properties of the molecular junction in the presence

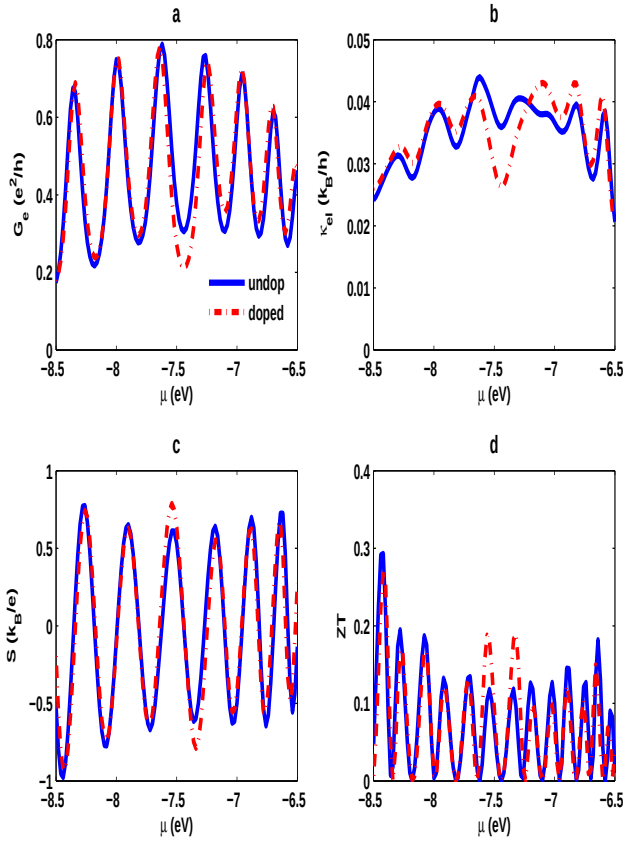

Fig. 7 Thermoelectric properties of polyaniline molecular junction a) electrical conductance, b) thermal conductance, c) thermopower and d) figure of merit, as a function of chemical potential of the electrodes for undoped and doped states. T=300k

and absence of dopants for the case of $n = 3$ via Fig. 7. The position of the chemical potential of the electrodes can be easily controlled by a bias. When the location of the chemical potential of the electrodes is changed the levels of the molecule participating in energy and charge transport can be changed. It is obvious from Figs. 7a-d, in vicinity of HOMO and LUMO levels, the two main levels taking part in transport mechanism, electrical and thermal conductances decrease due to doping process but the value of the thermopower increases. κ peaks are broadened with respect to G_e ones due to the effect of the temperature. The oscillation behavior of the thermopower denotes the change in population of the molecular energy levels [38–40]. The sign of the thermopower changes when the Fermi level crosses from electron-hole symmetry points and from resonance energies. Therefore, the thermopower is zero in these points [41]. In symmetry points, electrons and holes have the same weight in transport mechanism via opposite sign and the induced voltage drop is zero. In resonance energies, the carriers can tunnel from the colder and hotter electrodes to the molecular levels without needing thermal energy, so the themperature gradient cannot create a net electrical current and as a consequence the thermopower becomes zero. The figure of merit of the molecular junction in doped and undoped PANI junction is indicated in Fig. 7d. We observe that the ZT changes only in vicinity of HOMO and LUMO levels and increases in these energies during the doping process because of the identical behavior for the thermopower.

4 Conclusion

In this work, we have studied the thermoelectric properties of polyaniline (PANI) molecular junction in presence and absence of doping process using nonequilibrium Green function in linear response regime. The Hamiltonian of the molecule is described via the tight binding model and three dimensional semi-infinite FCC electrodes are used in the junction. The results provide a useful view to investigate doped-PANI as a thermoelectric material. Because the figure of merit of the junction increases in the presence of dopants as thermopower increases, but the electrical and thermal conductances decrease in doping process. In addition the thermoelectric properties of the PANI junction increase in higher temperatures and short lengths.

References

1 A. Malinauskas , *Polymer*, (2001), **42**, 3957173972, DOI:10.1016/S0032-3861(00)00800-4

2 A. Pron, P. Rannou, *Prog Polym Sci*, (2002), **27**, 135-190, DOI:10.1016/S0079-6700(01)00043-0.

3 A. Bhattacharya, A. De, *Prog Solid State Chem*, (1996), **24**, 141-181, DOI:10.1016/0079-6786(96)00002-7

4 Y. Zhaoa, G.S Tanga, Z.Z Yub, J.S Qic, *Carbon*. (2012), **50**, 3064173073, DOI:10.1016/j.carbon.2012.03.001

5 F. Mirjani, J. M. Thijssen, G. M. Whitesides, M. A. Ratner *ACS Nano*, (2014), **8**, 124281712436, DOI:10.1021/nn505115a.

6 K. Gupta, P.C. Janab, A.K. Meikap, *Solid State Sci.*, (2012), **14**, 32417329, DOI:10.1016/j.solidstatesciences.2011.12.003.

7 B. T. Raut, M. A. Chougule, A. A. Ghanwat, R. C. Pawar, C. S. Lee, V. B. Patil, *J. Mater. Sci-Mater. El.*, (2012), **23**, 2104-2109, DOI:10.1007/s10854-012-0708-7.

8 G.D. Khuspe, M.A. Chougule, S.T. Navale, S.A. Pawar, V.B. Patil, *Ceram. Int.*, (2014) **40**, 4267174276, DOI: 10.1016/j.ceramint.2013.08.091.

9 V. Bavastrello, T.B.C Terencio, C. Nicolini *Polymer*, (2011), **52**, 46-54, DOI: 10.1016/j.polymer.2010.10.022.

10 F. Yakuphanoglu, B. F. Şenkal *J. Phys. Chem. C*, (2007), **111**, 1840-1846. DOI: 10.1021/jp0653050.

11 M. Ghosh, A. Barman, S. K. De, and S. Chatterjee *J. Appl. Phys*., (1998), **84**, 806-811, DOI: dx.doi.org/10.1063/1.368141.

12 J. H. Jung, B. H. Kim, B. W. Moon, J. Joo, S. H. Chang, K. S. Ryu *Phys. Rev. B*, (2001), **64**, 035101-8, DOI: dx.doi.org/10.1103/PhysRevB.64.035101.

13 G. Lu, L. Bu, S. Li, X. Yang *Adv. Mater*., (2014), **26**, 2359-2364, DOI: 10.1002/adma.201305320.

14 W.B. Chang, Ch-K Mai, M. Kotiuga, J. B. Neaton,G. C. Bazan, R.A. Segalman,K. Maschke, *Chem. Mater.*, (2014), **26**, 7229-7235, DOI:dx.doi.org/10.1021/cm504254n.

15 X. F. Yang, Y. S. Liu, X. Zhang, L. P. Zhou, X. F. Wang, F. Chic, J. F. Feng, *Phys. Chem. Chem. Phys*, (2014), **16**, 11349-11355, DOI: 10.1039/c4cp00390j.

16 J. P. Bergfield, M. Solis, C. A. Stafford, *ACS Nano*, (2010), **4**, 5314-5320, DOI:10.1021/nn100490g.

17 H. Yan, N. Sada and N. Toshima, *J. Therm. Anal. Cal.*, (2002), **69**, 881-887, DOI: 10.1023/A:1020612123826.

18 B. Zheng, Y. Lin, J. Lan, X. Yang, *J. Mater. Sci. Technol*, (2014), **30**, 423-426, DOI: 10.1016/j.jmst.2013.11.008.

19 H. Yan, T. Ohta, N. Toshima *Macromol. Mater. Eng.*, (2001), **286**, 139-142, DOI: 10.1002/1439-2054(20010301)286:3 < 139::AID-MAME139 > 3.0.CO;2-F.

20 F. Yakuphanoglu, B. F. Şenkal, A. SaraÇ, *J. Electron. Mater*., (2008), **37**, 930-934, DOI: 10.1007/s11664-008-0404-9

21 A. Pud, N. Ogurtsov, A. Korzhenko, G. Shapoval, *Prog. Polym. Sci*., (2003), **28**, 1701-1753, DOI: 10.1016/j.progpolymsci.2003.08.001.

22 R. Hey, M. Schreiber, *J. Chem. Phys.*, (1995), **103**, 10726-10732, DOI: 10.1063/1.469859.

23 R. Hey, F. Gagel, M. Schreiber, *Phys. Rev. B*., (1997), **55**, 4231-4237, DOI: 10.1103/PhysRevB.55.4231.

24 S. Datta, *Quantum Transport: Atom to Transistor* (Cambridge University Press, Camberige, 2005).

25 Y. Asai, *Phys. Rev. B*., (2008), **78**, 045434-23 . DOI: 10.1103/PhysRevB.78.045434

26 M. Mrlik, M. Sedlacik, V. Pavlinek, P. Bober, M. Trchová, J. Stejskal, P. Saha, *Colloid Polym Sci*, (2013), **291**, 2079-2086 . DOI: 10.1007/s00396-013-2947-4.

27 Z. D. Zujovic, Y. Wang, G. A. Bowmaker, R. B. Kaner *Macromolecules*, (2011), **44**, 2735-2742, DOI: 10.1021/ma102772t.

28 Y. Meir, and N. S. Wingreen, *Phys. Rev. Lett*., (1992), **68**, 2512-2515. DOI: 10.1103/PhysRevLett.68.2512.

29 L. G. C. Rego, G. Kirczenow, *Phys. Rev. B*, (1999), **59**, 13080-13086, DOI:10.1103/PhysRevB.59.13080.

30 R. Y. Wang, R. A. Segalman, A. Majumdar, *App. Phys. Lett.*, (2006), **89**, 173113(1-3), DOI: 10.1063/1.2358856.

31 M. Brkle, T. J. Hellmuth, F. Pauly, Y. Asai, *arXiv:1503.02134*, (2015).

32 K. Baheti, J. A. Malen, P. Doak, P. Reddy, S-Y Jang, T. D. Tilley, A. Majumdar, R. A. Segalman, *Nano Lett.*, (2008), **8**, 715-719, DOI: 10.1021/nl0727381.

33 P. Reddy, S-Y Jang, R. A. Segalman, A. Majumdar, *SCIENCE*, (2007), **315**, 1568-1571, DOI: 10.1126/science.1137149

34 J. Li, X. Tang., H. Li, Y. Yan, Q. Zhang, *Synthetic Met.*, (2010), **160**, 1153-1158, DOI: 10.1016/j.synthmet.2010.03.001

35 Z. Golsanamlou, S. Izadi Vishkayi, M. Bagheri Tagani, H. Rahimpour Soleimani, *Chem. Phys. Lett.*, (2014), **594**, 51-57. DOI: 10.1016/j.cplett.2014.01.023.

36 Ch. Zeng, B. Li, B. Wang, H. Wang, K. Wang, J. Yang, J. G. Hou, Q. Zhu, *J. Chem. Phys.*, (2002), **117**, 851-856, DOI: 10.1063/1.1483846.

37 J. A. Malen, P. Doak, K. Baheti, T. D. Tilley, R. A. Segalman, A. Majumdar, *Nano Lett.*, (2009), **9** (3), 1164-1169, DOI: 10.1021/nl803814f.

38 M. Bagheri Tagani, and H. Rahimpour Soleimani, *J. Appl. Phys*., (2013), **113**, 143709-7. DOI: 10.1063/1.4800904.

39 M. B. Tagani, and H. R. Soleimani, *J. Appl. Phys*., (2012), **112**, 103719-7. DOI: 10.1063/1.4767376.

40 Z. Golsanamlou, S. Izadi Vishkayi, M. Bagheri Tagani, H. Rahimpour Soleimani, *NANO*, (2014), **9**, 1450057-13, DOI: 10.1142/S179329201450057X.

41 J. Zheng, F. Chi, Y. Guo, *J. Phy.: Condens. Matter*, (2012), **24**, 265301-8, DOI: 10.1088/0953-8984/24/26/265301.